Analytical small-signal theory of baritt diodes

Citation for published version (APA):
Roer, van de, T. G. (1974). *Analytical small-signal theory of baritt diodes*. (EUT report. E, Fac. of Electrical Engineering; Vol. 74-E-46). Technische Hogeschool Eindhoven.

Document status and date:
Published: 01/01/1974

Document Version:
Publisher’s PDF, also known as Version of Record (includes final page, issue and volume numbers)

Please check the document version of this publication:

- A submitted manuscript is the version of the article upon submission and before peer-review. There can be important differences between the submitted version and the official published version of record. People interested in the research are advised to contact the author for the final version of the publication, or visit the DOI to the publisher's website.
- The final author version and the galley proof are versions of the publication after peer review.
- The final published version features the final layout of the paper including the volume, issue and page numbers.

Link to publication

General rights
Copyright and moral rights for the publications made accessible in the public portal are retained by the authors and/or other copyright owners and it is a condition of accessing publications that users recognise and abide by the legal requirements associated with these rights.

- Users may download and print one copy of any publication from the public portal for the purpose of private study or research.
- You may not further distribute the material or use it for any profit-making activity or commercial gain
- You may freely distribute the URL identifying the publication in the public portal.

If the publication is distributed under the terms of Article 25fa of the Dutch Copyright Act, indicated by the “Taverne” license above, please follow below link for the End User Agreement:

www.tue.nl/taverne

Take down policy
If you believe that this document breaches copyright please contact us at:

openaccess@tue.nl

providing details and we will investigate your claim.

Download date: 27. Feb. 2021

ANALYTICAL SMALL-SIGNAL THEORY OF BARITT DIODES

by

Th. G. van de Roer

Department of Electrical Engineering
Eindhoven University of Technology
Eindhoven, The Netherlands

ANALYTICAL SMALL-SIGNAL THEORY OF BARITT DIODES

by

Th. G. van de Roer

TH-Report 74-E-46

May 1974

ISBN 90 6144 046 7

ABSTRACT

An analytical theory for the small-signal impedance and noise of Baritt- (or punch-through) diodes is presented. The diode is divided into three regions. In the two regions closest to the injecting contact the effects of thermionic injection and diffusion are accounted for in an approximate way. In the remaining region diffusion is neglected but an otherwise exact solution is given for an arbitrary relationship between drift velocity and electric field. Results of the calculations are presented in graphical form and the influence of the parameters frequency, d.c. current, temperature and impurity concentration is discussed.

CONTENTS Page

I. Introduction

Since Shockley [1] first proposed the use of punch-through diodes as negative-resistance devices for microwave frequencies, a number of papers has appeared treating the d.c. and small signal a.c. theory of these devices. Especially since the first experimental realization by Coleman and Sze [2], the interest in punch-through diodes, and with it the number of papers about them, have increased strongly.

Yoshimura [3] has given solutions for the d.c. and small signal a.c. impedances for the case where the mobility is constant throughout the diode. Wright [4], Weller [5], Coleman [6] and Haus et. al. [7] have published theories for the case of saturated drift velocity throughout the device, the main difference between their theories being the boundary conditions applied at the injecting contact. Vlaardingerbroek and the author [8] have pointed out the importance of the combination of a non-saturated and a saturated region.

Finally, a number of numerical calculations have been published [9,10,11,12]. The small-signal noise properties have been discussed in some of the above-mentioned papers as well as in a few others [7,12,13,14,15,16].

In the analytical theories published hitherto, diffusion effects on the small-signal impedance have been neglected or represented by a modified boundary condition. An exact analysis would require the solution of a second-order differential equation with variable constants which can only be done numerically. It is felt, however, that incorporating diffusion in an analytical theory, although approximate, is still worthwile because it can give more insight than a numerical analysis. To do this is the scope of this investigation of which preliminary results already have been published [17].

The approach chosen here relies on the fact that the electric field rises steadily from the injecting contact to the other one while the carrier density decreases simultaneously. One may then assume that near the injecting contact the main factors governing carrier transport will be thermionic injection and diffusion whereas in the region of higher field strength the electric field will be dominant.

The diode is divided into three regions:

i. the contact region where thermionic injection prevails. This region lies between the injecting contact and the point of zero electric field (potential maximum).

ii. the diffusion region where carrier transport is by diffusion mainly. This region stretches from the potential maximum to a point where the d.c. field has risen to such a value that diffusion may be neglected. Necessarily the choice of this point will be somewhat arbitrary.

iii. the drift region, comprising the rest of the diode, where the electric field is dominant.

The analysis will start with the drift region and then work its way back to the injecting contact. This is done because the drift region makes up the greatest part of the diode and it can be treated without approximations. The properties of the diode can then be discussed in terms of the boundary conditions at the input of the drift region, which in turn are determined by the injecting contact and the diffusion region.

The small-signal noise properties will be discussed after the impedance. Shot noise and thermal noise will be taken as the only noise sources.

In the last section some numerical results and comparison with experiments will be presented.

II- General

Consider a planar semiconductor structure consisting of a layer of n-type material sandwiched between two metal (or p+) contacts (fig. 1). The p+(metal) layers form rectifying contacts (Schottky-barriers) and consequently narrow depletion layers are formed at both contacts. When a d.c. voltage is applied with the plus on the left hand contact, the right hand depletion layer will widen but the device draws no current. This goes on until the two depletion layers meet, a situation called reach-through or punch-through. The field and potential distributions are now as shown in fig. 2. Also shown is the energy band diagram. Any hole that now is injected from the left hand contact with sufficient energy to cross the potential barrier is picked up by the field and transported to the other side. When the voltage now is increased the potential barrier is reduced and the current increases sharply. It is this feature of the punch-through diode that makes its operation as a high-frequency negative-resistance device possible.

For the analysis reference is made to fig. 3. The variables to be considered are:

the total current density J
the electric field E
the drift velocity v

which are all three in the x-direction, and

the hole density p.

All these are assumed to be functions of the space coordinate x and to consist of a large d.c. part (with index 0) and a small a.c. part (index 1) with time dependence $\exp(j\omega t)$.

Also entering the equations are the donor density N_D, taken constant over the length of the diode, and the dielectric constant ε of the semiconductor material.

The position of x_i is defined by specifying the value E_i the d.c. electric field has attained at this point. It will be in the order of several kilovolts per cm.

It will be convenient to use reduced quantities. These are defined as follows.

$$\eta = \frac{E}{E_S}\ , \quad i = \frac{J}{\sigma E_S}\ , \quad \nu = \frac{v}{v_s}\ , \quad \xi = \frac{eN_D}{\varepsilon E_s}\,x \text{ and } \alpha = \frac{\omega\varepsilon}{\sigma} \qquad (1)$$

with $E_s = \frac{v_s}{\mu_o}$ and $\sigma = e\mu_o N_D$, e being the elementary unit of charge.
In priciple v_s and μ_o are arbitrary scaling factors. The most natural, however, is to take for v_s the value of the saturated drift velocity and for μ_o the low-field mobility.

III The small-signal Impedance

III-1. The drift region

In this region the drift velocity is a function of the electric field only. The total current density is no function of x and is given by:

$$J = e.p.v(E) + \varepsilon\ .\ \frac{\partial E}{\partial t} \qquad (3)$$

The field is given by Poisson's equation:

$$\frac{\partial E}{\partial x} = \frac{e}{\varepsilon}\,(N_D + p) \tag{4}$$

In reduced form these equations read:

$$i = \frac{p}{N_D}\nu + \frac{\varepsilon}{\sigma}\frac{\partial \eta}{\partial t} \tag{3a}$$

$$\frac{\partial \eta}{\partial \xi} = 1 + \frac{p}{N_D} \tag{4a}$$

The equations are now split in their d.c. and a.c. parts which are solved separately. The a.c. equations are linearized assuming the a.c. quantities to be small.

III-1.1. D.C. Solution

The d.c. parts of (3a) and (4a) yield, eliminating p:

$$i_o = -\nu_o + \nu_o\frac{d\eta_o}{d\xi} \tag{5}$$

With the boundary condition $\eta = \eta_i = \frac{E_i}{E_s}$ at $x = x_i$ one can write the solution of (5) as:

$$\xi = \int_{\eta_i}^{\eta_o} \frac{\nu_o(\eta)}{i_o + \nu_o(\eta)}\,d\eta + \xi_i . \tag{6}$$

The d.c. voltage over the drift region can also be found directly:

$$V_{od} = \int_{x_i}^{\ell} E_o dx = \frac{\varepsilon E_s^2}{eN_D}\int_{\eta_i}^{\eta_d} \frac{\eta.\nu_o(\eta)}{i_o + \nu_o(\eta)}\,d\eta \tag{7}$$

where η_d is the value of η_o at $x = \ell$.

III-1.2. A.C. Solution

A first order pertubation analysis is applied to find the a.c. components. The a.c. component of ν is obtained from a Taylor-series expansion:

$$\nu_1 = \frac{d\nu_o}{d\eta_o}\,\eta_1 . \tag{8}$$

Combining (1) and (2) and eliminating the d.c. terms gives in reduced form:

$$i_1 = (j\alpha + \frac{i_o}{\nu_o}\frac{d\nu_o}{d\eta_o})\eta_1 + \nu_o\frac{d\eta_1}{d\xi} \quad . \tag{9}$$

This is most easily solved by converting to a new independent variable τ defined by:

$$\tau = \int_{\xi_i}^{\xi}\frac{d\xi'}{\nu_o(\xi')} \quad . \tag{10}$$

Evidently τ is the transit-time of a hole from x_i to x, divided by the dielectric relaxation time ε/σ.

Substituting (10) eq. (9) becomes:

$$i_1 = (j\alpha + \frac{i_o}{\nu_o}\frac{d\nu_o}{d\eta_o})\eta_1 + \frac{d\eta_1}{d\tau} \quad . \tag{11}$$

The general solution of the homogeneous form ($i_1 = 0$) of (11) is well known. It reads:

$$\eta_{1h} = \exp - \int_o^{\tau}(j\alpha + \frac{i_o}{\nu_o'}\frac{d\nu_o'}{d\eta_o'})d\tau' \quad . \tag{12}$$

Using (4a) and (10) this can be simplified to:

$$\eta_{1h} = (1 + \frac{i_o}{\nu_o})\exp{-j\alpha\tau} \tag{13}$$

The complete solution of (11) now can be found by substituting $\eta_1 = \eta_{1h}F(\tau)$ and solving for F. The boundary condition for η_1 at $\tau = 0$ ($x = x_i$) is formally put down as

$$\eta_1(0) = \rho_i i_1$$

where ρ_i has to be determined from an analysis of the preceding region.

The following expression then is obtained:

$$\eta_1(\tau) = i_1\left(1 + \frac{i_o}{\nu_o}\right)\exp -j\alpha\tau\left[\frac{\rho_i\nu_i}{i_o + \nu_i} + \int_0^{\tau} \frac{\nu_o'}{i_o + \nu_o'}\exp j\alpha\tau' d\tau'\right] . \qquad (14)$$

Here $\nu_i = \nu_o(\eta_i)$.

Calculation of the a.c. impedance Z_d of the drift region now is straightforward. With A the diode area and $\tau_\ell = \tau(\ell)$ we have:

$$Z_d = \frac{1}{J_1 A}\int_{x_i}^{\ell} E_1 dx = Z_o\int_0^{\tau_\ell}\frac{\nu_o\eta_1}{i_1}d\tau$$

$$\text{with } Z_o = \frac{\varepsilon v_s}{\sigma^2 A} \qquad (15)$$

Substituting (14) one obtains:

$$Z_d = Z_o\int_0^{\tau_\ell}(i_o + \nu_o)\exp -j\alpha\tau\left\{\frac{\rho_i\nu_i}{i_o + \nu_i} + \int_0^{\tau}\frac{\nu_o'}{i_o + \nu_o'}\exp j\alpha\tau' d\tau'\right\}d\tau \qquad (16)$$

A similar expression valid for majority-carrier current (Gunn-diodes) has been obtained by Dascalu [18]. This expression is obtained from (16) by changing the sign of i_o.

III-1.3 Discussion

Expression (16) can be evaluated further without specifying the v-E-relationship. In the following this has been done in such a way that the influence of the non-saturated part of the drift region is separated out. One then arrives at the expression:

$$\frac{Z_d}{Z_o} = \frac{\xi_\ell - \xi_i}{j\alpha} + \frac{\nu_i(1+i_o)}{\nu_i + i_o}\left\{\rho_i - \frac{1}{j\alpha}\right\}\frac{1-\exp -j\alpha\tau_\ell}{j\alpha} +$$

$$- \frac{\nu_i}{\nu_i + i_o}\left\{\rho_i - \frac{1}{j\alpha}\right\}\int_0^{\tau_\ell}(1 - \nu_o)\exp -j\alpha\tau d\tau \quad +$$

$$- \frac{i_o}{j\alpha}\int_0^{\tau_\ell}(i_o+\nu_o)\exp -j\alpha\tau d\tau\int_0^{\tau}\frac{\exp j\alpha\tau'}{\nu_o' + i_o}\,\frac{d\nu_o'}{d\eta_o'}d\tau' \qquad (17)$$

(17) can be interpreted as follows:
the first term clearly represents the lattice capacitance of the drift space. The last two terms are zero if the drift velocity is saturated throughout the drift region.
In this case to obtain a negative resistance ρ_i must satisfy the condition $\arg (\rho_i + \frac{1}{\alpha}) \neq \frac{\pi}{2}$.

In Impatt diodes $\arg (\rho_i + \frac{j}{\alpha}) = - \frac{\pi}{2}$ when the signal frequency is above the avalanche frequency which is the optimal condition for negative resistance. In Baritt-diodes ρ_i has a positive real part in most cases and negative resistance in possible too.

However, even in case $\arg (\rho_i + \frac{j}{\alpha}) = \frac{\pi}{2}$ the third and fourth term of the r.h.s. of (17) may contribute a negative real part when the drift velocity is not saturated, as has been pointed out in [8] for a specific v-E-relationship. A general proof is hard to give but looking at the third term it can be seen that when $1 - \nu_o$ is a monotonously decreasing function of τ (which is the case when ν_o increases monotonously with η_o) and when $1 - \nu_o(\tau_\ell)$ is so small that the upper limit can be extended to infinity the integral has a negative imaginary part so that the whole third term has a negative real part.

III-2 The diffusion region

III-2.1 A.C. Solution

The carrier transport in this region is governed to a large extent by diffusion. An exact analysis would require the solution of second-order non-linear differential equations, which in general can only be done by numerical methods. In this work we will restrict ourselves to a simplified analysis, which although less exact, can provide better insight than a numerical calculation.

The drift velocity now is given by:

$v = v(E) - \frac{D}{p}\frac{\partial p}{\partial x}$ where D is the diffusion constant. In reduced form this becomes

$$\nu = \nu(\eta) - \frac{\delta}{p}\frac{\partial p}{\partial \xi} \tag{18}$$

$$\text{where } \delta = \frac{\sigma D}{\varepsilon v_s^2} \tag{19}$$

which together with (1), (2), (3) and (7) gives for the a.c. quantities:

$$i_1 = (j\alpha + \frac{i_o}{\nu_o}\frac{d\nu_o}{d\eta_o})\,\eta_1 + \nu_o\frac{d\eta_1}{d\xi} - \delta\frac{d^2\eta_1}{d\xi^2} \tag{20}$$

This equation is simplified by replacing ν_o by an average value ν_a and assuming the mobility constant at its low-field value so $\frac{d\nu_o}{d\eta} = 1$. The solution of (20) then becomes:

$$\eta_1 = i_1\{B_o + B_1\exp-\gamma_1(\xi - \xi_m) + B_2\exp\gamma_2(\xi - \xi_i)\} \tag{21}$$

with

$$B_o = {}^1\!/(i_o/\nu_a + j\alpha) \tag{22}$$

$$\gamma_{1,2} = \frac{\nu_a}{2\delta}\left\{\mp 1 + \sqrt{1 + \frac{4\delta}{\nu_a^2}(\frac{i_o}{\nu_a} + j\alpha)}\right\} \tag{23}$$

Eq. (21) reveals the existence of two waves, one forward travelling with amplitudecoefficient B_1 and one backward travelling with amplitude B_2. The latter usually is called a diffusion wave because it does not show up in an analysis where diffusion is neglected. But even in the present case it is doubtful that this wave will be excited. The point where it would be excited, x_i, is an artificial boundary created to simplify the analysis but not existing in reality. Therefore it is considered appropriate, although it is not correct mathematically, to leave out this wave so that the influence of diffusion only is to change the character of the forward wave.

The amplitude B_1 then is found by matching the field at x_m. It is assumed that the relation between field and current density can be written as:

$$i_1 = (\sigma_c + j\alpha) \cdot \eta_1(\xi_m) \tag{24}$$

where σ_c has to be found from an analysis of the contact region. Section III-3 will be devoted to this analysis.

For B_1 one thus finds:

$$B_1 = \frac{1}{\sigma_c + j\alpha} - B_o \tag{25}$$

Finally, the impedance Z_i of the diffusion region and the boundary condition parameter ρ_i are found as:

$$Z_i = \frac{\varepsilon}{\sigma C_i} B_o - B_1 \frac{\exp-\gamma_1(\xi_i - \xi_m) - 1}{\gamma_1(\xi_i - \xi_m)} \tag{26}$$

$$\rho_i = B_o + B_1 \exp-\gamma_1(\xi_i - \xi_m) \tag{27}$$

where $C_i = \dfrac{\varepsilon A}{x_i - x_m}$ is the "cold" capacitance of the diffusion region.

III-2.2 D.C. Solution

The quantities $\xi_i - \xi_m$ and ν_a, occurring in the preceding paragraph, have to be found from a d.c. analysis. Again, approximations have to be introduced because of the non-linearity of the equations. The approximation used now is that the d.c. current is carried by diffusion only. This gives:

$$i_o = -\frac{\delta}{N_D}\frac{dp_o}{d\xi} . \tag{28}$$

With the boundary condition that p_o be continuous at x_i the solution of (28) is:

$$\frac{p_o}{N_D} = \frac{i_o}{\nu_i} - \frac{i_o}{\delta}(\xi - \xi_i) \tag{29}$$

With Poisson's equation then the electric field is found:

$$\eta_o = (1 + \frac{i_o}{\nu_i} + \frac{i_o\xi_i}{\delta})(\xi - \xi_m) - \frac{i_o}{2\delta}(\xi - \xi_m)^2 \tag{30}$$

Demanding continuity of E_o at x_i then yields $\xi_i - \xi_m$:

$$\xi_i - \xi_m = \frac{\delta}{i_o}\left\{-1 - \frac{i_o}{\nu_i} + \sqrt{\left(1 + \frac{i_o}{\nu_i}\right)^2 + \frac{2\eta_i i_o}{\delta}}\right\} \tag{31}$$

The average reduced drift-velocity is defined such that it gives the same transit-time from x_m to x_i as the non-averaged velocity:

$$\frac{\xi_i - \xi_m}{\nu_a} = \int_{\xi_m}^{\xi_i} \frac{d\xi}{\nu_o} \quad \text{which gives for } \nu_a:$$

$$\nu_a = \frac{\nu_i}{1 + \dfrac{\nu_i(\xi_i - \xi_m)}{2\,\delta}} \tag{32}$$

III-2.3 Discussion

Eq. (21) can, using (25), be written as:

$$\eta_1 = i_1\left[(B_o+B_1)\exp -\gamma_1(\xi-\xi_m) + B_o\left\{1 - \exp -\gamma_1(\xi-\xi_m)\right\}\right] \tag{33}$$

Apparently η_1 consists of a constant term and and a wave propagating in the direction of the drift which is damped by velocity modulation and diffusion. The result of the damping is that as the wave progresses the influence of the contact region, represented by the first term in (33), is decreased whereas the influence of the injection region itself increases. The result is that, depending on the degree of damping, the contact region is more or less screened off by the injection region. Situations are possible, however, where there is hardly any screening at all. Specifically, when $\sigma_c \approx \frac{i_o}{\nu_a}$ the amplitude of the wave is small and the a.c. electric field is constant throughout the injection region. In this case the boundary condition (24) can be applied without modification at x_i.

III-3 The contact region

The contact region is analysed under the assumption that the flat-band situation is not reached, i.e. the zero-electric-field point (potential-minimum) lies at a finite distance from the contact. Numerical analysis [15,21] has shown that in m-s-m diodes flat-band can be reached at relatively low current densities so that in this case our analysis is not valid for high current densities. On the other hand, the screening effect described in the previous section becomes more pronounced at higher current densities, so the error introduced probably remains small.

For the following derivation reference is made to fig. 3. The d.c. hole distribution for $x < x_m$ is given by:

$$p_o = N_v \exp - \frac{V + \psi'_m}{V_T} \quad \text{with } V_T = \frac{kT}{e} \tag{34}$$

$$\text{Define } \phi = \frac{V}{V_T} \quad \lambda_D^2 = \frac{\varepsilon V_T}{eN_D} \quad \text{and} \quad \xi = \frac{x}{\lambda_D} \tag{35}$$

Then Poisson's equation gives:

$$\frac{d^2\phi}{d\xi^2} = -1 - \zeta \exp - \phi \tag{36}$$

$$\text{with } \zeta = \frac{N_v}{N_D} \exp - \frac{\psi'_m}{V_T} \tag{37}$$

Writing $\frac{d^2\phi}{d\xi^2} = \frac{1}{2} \frac{d}{d\phi} \left(\frac{d\phi}{d\xi}\right)^2$ one can integrate (32) to:

$$\xi_m = \int_0^{\phi_m} \frac{d\phi}{\{2(\phi_m - \phi + \zeta \exp - \phi - \zeta \exp - \phi_m)\}^{\frac{1}{2}}} \tag{38}$$

The largest contribution comes from the region $\phi \approx \phi_m$ where the integrand has an integrable singularity, so substitute

$$\exp(\phi_m - \phi) = 1 + \phi_m - \phi$$

Then one finds

$$\xi_m = \left(\frac{2\phi_m}{1 + \zeta \exp - \phi_m}\right)^{\frac{1}{2}} \tag{39}$$

ϕ_m is calculated from the thermionic emission formula:

$$J_o = J_{so} \exp - \phi_m \tag{40}$$

The quantity σ_c introduced in the preceding section is calculated the same way as by Haus et.al. [7] , viz. by a perturbation of (36) assuming the a.c. convection current to be small compared to the dielectric current. The result is:

$$\sigma_c = \frac{J_o x_m}{\sigma V_T} \tag{41}$$

The a.c. voltage drop over the contact region is equal to $E_1 x_m$ so that the impedance of the contact region becomes:

$$Z_c = \frac{x_m}{\sigma(\sigma_c + j\alpha)A} = Z_o \frac{\xi_m}{\sigma_c + j\alpha} \tag{42}$$

IV - Noise Properties

IV-1. Introduction

To discuss the small-signal noise properties of Baritt-diodes the open-circuit noise voltage V_N is calculated. From this a noise measure M can be defined by the following expression:

$$M = \frac{\overline{V_N^2}}{4kT|\mathrm{Re}\ Z_1|} \tag{43}$$

M is directly related to the noise figure F of a reflection-amplifier using the diode [19]. The relationship can be expressed as follows:

$$F = 1 + M(1 - \frac{1}{G}) \tag{44}$$

where G is the gain of the amplifier.

In a Baritt-diode, where carrier multiplication and intervalley-scattering are absent, the main sources of noise are:

shot noise, originating in statistical fluctuations of the injected carrier current, and

thermal nois due to random thermal motion of the carriers.

The shot noise will be calculated following the method of Haus et.al. [7]. For the thermal noise the impedance-field method will be used [13,20].

IV-2. Shot noise

The shot noise is calculated under the assumption that at $x = x_m$ a noise current J_s is injected whose mean square amplitude is given by the well known formula

$$\overline{I_s^2} = 2eJ_oA\Delta f \quad , \tag{45}$$

To obtain the open-circuit noise voltage we have to solve for the a.c. electric field under the assumption that the total current J_1 is zero. So at x_m the sum of injected current and field-induced current has to be zero:

$$i_s + (\sigma_c + j\alpha)\cdot\eta(\xi_m) = 0 \tag{46}$$

$$\text{where } i_s = \frac{I_s}{\sigma E_s A} \; . \tag{47}$$

In the diffusion region we now have with (46)

$$\eta_s = \frac{-i_s}{\sigma_c + j\alpha} \exp\{-\gamma_1(\xi - \xi_m)\} \tag{48}$$

From this the noise voltage over the diffusion region follows:

$$V_{si} = Z_o I_s \; \frac{\exp\{-\gamma_1(\xi_i - \xi_m)\} - 1}{(\sigma_c + j\alpha)\;\gamma_1} \tag{49}$$

Equation (48) also gives us the boundary condition for the drift region by inserting $\xi = \xi_i$. In the drift region we then have:

$$\eta_s = \frac{-\,i_s}{\sigma_c + j\alpha} \exp\{-\gamma_1(\xi_i - \xi_m) \; \frac{\nu_i}{\nu_i + i_o} \cdot \frac{\nu_o + i_o}{\nu_o} \exp - j\alpha\tau \tag{50}$$

The noise voltage over this region thus becomes:

$$V_{sd} = -\, Z_o I_s \exp\{-\gamma_1(\xi_i - \xi_m)\} \; \frac{\nu_i}{\nu_i + i_o} \int_0^{\tau_\ell} (\nu_o + i_o) \exp - j\alpha\tau \; d\tau \tag{51}$$

IV-3. Thermal noise

IV-3.1. Introduction

The thermal noise is calculated with the impedance-field method [20] . It gives the expression:

$$\overline{V^2_{th}} = 4e^2 A \int_0^{\ell} \left| \frac{dZ_{TX}}{dx} \right|^2 D(x) \; . \; p_o(x) \; dx \; . \; \Delta f \tag{52}$$

Here D(x) is a quantity dependent on the specific noise-generation mechanism considered. For thermal noise it can be identified with the diffusion constant D.

The quantity $\frac{dZ_{TX}}{dx}$ is the impedance-field vector. Its meaning is illustrated by fig. 4.

Suppose a noise current δI_N is injected at a plane X and extracted again at a plane X + ΔX. This current produces a voltage δV_N across the terminals of the diode. Now the impedance-field is defined by

$$\frac{dZ_{TX}}{dx} = \frac{\delta V_N}{\delta I_N} \tag{53}$$

Assuming that the noise currents in the different parts of the diode are uncorrelated the noise voltages have to be summed quadratically which leads to (52). Evidently in this formula D(x) represents the actual nature of the noise current whereas $\frac{dZ_{TX}}{dx}$ relates to the way this current produces a voltage across the terminals.

To obtain $\frac{dZ_{TX}}{dx}$ one has to solve the same equations as before but assuming a total current δI_N between X and X + dX and zero total current in the rest of the diode.

IV-3.2. Diffusion region

When the plane X is in the diffusion region we assume the following fields to exist (X_r is the reduced value of X): For $\xi_m < \xi < X_r$ a backward traveling wave:

$$\eta_t = A \exp \gamma_2 \xi \tag{54}$$

For $X_r < \xi < X_r + \Delta X_r$ the complete solution of the inhomogeneous differential equation:

$$\eta_t = \delta i_t (B_o + B_1 \exp - \gamma_1 \xi + B_2 \exp \gamma_2 \xi) \tag{55}$$

where δi_t is the reduced injected noise current and B_o has the same value as in section III-2. For $X_r + \Delta X_r < \xi < \xi_i$ a forward travelling wave:

$$\eta_t = C \exp -\gamma_1 \xi \quad . \tag{56}$$

The backward wave in this region is neglected on the same grounds as in III-2.

Imposing continuity of η_1 and $\frac{d\eta_1}{d\xi}$ at X_r and $X_r + \Delta X_r$ we find in the limit $\Delta X_r \to 0$:

$$C = B_o \frac{\gamma_1 \gamma_2}{\gamma_1 + \gamma_2} \exp \gamma_1 X_r \cdot \delta i_t \, \Delta X_r \tag{57}$$

The calculation of the impedance-field is simplified considerably if we assume that the voltage drop across the diffusion region itself may be neglected, the diffusion region being short compared to the drift region, so that the voltage across the latter only has to be calculated. The boundary condition for the drift region follows from (56) and (57).

The final result is:

$$\frac{\Delta Z_{Tx}}{\Delta x} (\xi_m < X_r < \xi_i) = \frac{1}{\sigma A} B_o \frac{\gamma_1 \gamma_2}{\gamma_1 + \gamma_2} \exp\{-\gamma_1 (\xi_i - X_r) . \frac{\nu_i}{\nu_i + i_o} \int_o^{\tau_\ell} (\nu_o + i_o) \exp -j\alpha\tau d\tau \tag{58}$$

IV-3.3. Drift region

When X_r is in the drift region we assume as before that only one, forward traveling, wave exists. Then for $\xi < X_r$ there is no electric field. For $X_r < \xi < X_r + \Delta X_r$ we have the differential equation:

$$\delta i_t = (j\alpha + \frac{i_o}{\nu_o} \frac{d\nu_o}{d\eta_o}) \eta_1 + \frac{d\eta_1}{d\tau} \tag{59}$$

As $\eta_1 = 0$ at X_r the contribution of the term with η_1 in the above equation is of second order, so we find for the field at $X_r + \Delta X_r$:

$$\eta_1 (X_r + \Delta X_r) = \frac{d\eta_1}{d\xi} . \Delta X_r = \frac{1}{\nu_o(X_r)} \delta i_t \Delta X_r \tag{60}$$

All we have to do now is calculate the field in the region $\xi > X_r$ and integrate to obtain the noise voltage. The result is:

$$\frac{dZ_{Tx}}{dx} = \frac{1}{\sigma A} \frac{\exp j\alpha\tau_x}{\nu_o(\tau_x)+i_o} \int_{\tau_x}^{\tau_\ell} (\nu_o + i_o) \exp -j\alpha\tau d\tau , \tag{61}$$

where $\tau_x = \tau(X_r)$

IV-3.4. Discussion

From the expressions for the noise voltage derived in the preceding section it is hard to draw any general conclusions. However, one may note that (51) and (58) lead to terms of the same form in the expressions for the mean square voltage. If we take (51) and (58) as representative for the shot noise and the thermal noise, respectively, then we are able to get an impression of the relative magnitude of both noise sources. Taking the square of the absolute value of (51) and substituting (58) in (52) and dividing the results we obtain:

$$\frac{\overline{V^2_{th}}}{\overline{V^2_s}} \approx \frac{2\delta}{\nu_a} \left| \frac{B_o\gamma_1\gamma_2}{\gamma_1+\gamma_2} \right|^2 \frac{\exp 2 \operatorname{Re} \gamma_1(\xi_i-\xi_m) - 1}{2 \operatorname{Re} \gamma_1} \tag{62}$$

Substituting B_o, γ_1 and γ_2 this reduces to:

$$\frac{\overline{V^2_{th}}}{\overline{V^2_s}} \approx \frac{2\,\delta}{\nu_a^3 \{(1+\frac{4\delta i_o}{\nu_a^3})^2 + (\frac{4\delta\alpha}{\nu_a^2})^2\}} \cdot \frac{\exp 2 \operatorname{Re} \gamma_1(\xi_i - \xi_m) - 1}{2 \operatorname{Re} \gamma_1} \tag{63}$$

Inserting representative numbers e.g.:

$N_D = 10^{21}$ m^{-3} $\qquad$ $D = 10^{-3}$ m^2 s^{-1}

$\mu = 0.05$ m^2 V^{-1}s^{-1} $\qquad$ $\nu_i = 0.4$

$v_s = 10^5$ m s^{-1} $\qquad$ $\varepsilon = 10^{-10}$ A s V^{-1} m^{-1}

we find at low current densities: $\delta = 0.008$ and $\nu_a = 0.03$ so that the first factor of (63) is a large number whereas the second factor is in the order of one. At increasing current densities the first factor decreases but the second one increases. One might therefore conclude that the thermal noise is the dominant noise source at all current densities.

V Numerical Results

For a numerical calculation the v-E-relationship must be specified. The measured v-E-characteristics of Canali et.al. [22] were used as a starting point. They can very well be approximated by the function:

$$v = \frac{\mu_o E}{1 + \frac{\mu_o E}{v_s}} \tag{64}$$

For instance, at room temperature one finds $\mu_o = 450\ \mathrm{cm}^2/\mathrm{Vs}$ and $v_s = 0.9.10^7$ cm/s.

Unfortunally it is not possible to evaluate the expressions for impedance and noise obtained in the previous sections for this v-E-relationship. Therefore the curve has been approximated by three straight lines (fig. 5). The first intersection is chosen at the electric field E_i, which also marks the end of the diffusion region. When the values of μ_o, v_s and E_i have been selected, the value of μ_2 is taken such that at zero d.c. current the transit-time from x_i to ℓ is the same as it would be for the v-E-relationship of (64).

First it was tried to reproduce the experimental results of Bjorkman and Snapp [23]. The following parameter values were used:

$\mu_o = 450\ \mathrm{cm}^2/\mathrm{Vs}$
$v_s = 0.075 \cdot 10^7$ cm/s
$E_i = 7$ kV/cm
$A = 3.10^{-4}\ \mathrm{cm}^2$
$\ell = 7.9\ \mu\mathrm{m}$
$N_D = 1.2.10^{15}\ \mathrm{cm}^{-3}$
$T = 17^\circ$ C
$\varepsilon = 12\varepsilon_o$

The results are shown in fig. 6. It turns out that the agreement is good at the low current of 5 mA but at the higher currents the calculated values of the negative conductance are higher and occur at higher frequencies than the measured ones.

One might wonder what influence the parameter E_i has on the result. An impression of this influence is given in fig. 7 where E_i is varied from 6 to 8 kV/cm with the d.c. current at 5 mA. Evidently there is an appreciable influence. At higher currents however the change of the curves with E_i becomes less and at 40 mA it is insignificant.

As a second step it was tried to find out if the temperature rise of the diode at high currents could be responsible for the discrepancy between theory and experiment. The temperature enters explicitly in the formulas for the contact region. Furthermore it is assumed that the low-field mobility varies as:

$$\mu_o = \mu_{o,T_o}\left(\frac{T}{T_o}\right)^{-2,3} \tag{65}$$

From the data given in [22] one may conclude that the saturated drift velocity varies little with temperature, so it was held constant. The diffusion constant too was kept constant.

The results of this calculation are shown in fig. 8 for currents of 20 and 40 mA and various temperatures. Evidently the frequency shift (or better the lack of frequency shift) of the negative conductance can be explained by a temperature change but not the variation of the magnitude of the negative conductance. Not shown is the variation of the susceptance. It decreases with increasing current, but increases with increasing temperature.

Finally, the influence of donor density was examined. A typical result is shown in fig. 9 for a current of 20 mA and a temperature of 50° C. Two conclusions may be drawn from this figure: firstly, the frequency region of negative conductance shifts to higher frequencies with increasing donor density and secondly, the magnitude of the negative conductance decreases sharply when the donor density drops below a certain value. Further investigation showed that the last phenomenon is dependent on the length of the diode and it seems that there is something like a minimum $N_D\ell$ product for good operation of this type of diode.

VI Conclusion

An analytical theory for the small-signal characteristics of Baritt-diodes has been developed. It takes into account the influences of the non-saturated drift velocity, diffusion and the properties of the injecting contact.

The theory gives insight into the physical behaviour of the diode as well as numerical values for the impedance and noise that fit well to experimental results.

Some important results are:

i. the region of negative resistance shifts to higher frequencies with increasing current, but to lower frequencies with increasing temperature. A similar feature in the susceptance could be useful for stabilization of Baritt oscillators.

ii. the region of negative resistance shifts to higher frequencies with increasing donor density. A minimum density (at a given diode length) is necessary to obtain a useful negative resistance.

iii. thermal noise is the dominant noise source.

REFERENCES

[1]. W. Shockley - BSTJ 33, 799-826 (1954).

[2]. D.J. Coleman, S.M.Sze - BSTJ 50, 1695-1699 (1971).

[3]. H. Yoshimura - IEEE Trans. ED-11, 414-422 (1964).

[4]. G.T. Wright - Electron. Lett. 7, 449-451 (1971).

[5]. K.P. Weller - RCA Rev. 32, 373-382 (1971).

[6]. D.J. Coleman - J.A.P. 43, 1812-1818 (1972).

[7]. H.A. Haus, H. Statz, R.A. Pucel - Electron.Lett. 7, 667-669 (1971).

[8]. M.T. Vlaardingerbroek, T.G. v.d. Roer - Appl. Phys. Lett. 22, 146-148 (1973).

[9]. E.P. Eer Nisse - Appl. Phys. Lett., 20, 301-304 (1972).

[10]. J.A.C. Stewart, J. Wakefield - Electron. Lett. 8, 378-379 (1972).

[11]. M. Matsumura - IEEE Trans. ED-19, 1131-1133 (1972).

[12]. A. Sjölund - Solid State El. 16, 559-569 (1973).

[13]. H. Statz, R.A. Pucel, H.A. Haus - Proc. IEEE 60, 644-645 (1972).

[14]. A. Sjölund - Electron. Lett. 9, 2 - (1973).

[15]. J. Christie, B.M. Armstrong, J.A.C. Stewart - Proc. 1973 European Microwave Conference, A.10.2 (Brussels, 1973).

[16]. A. Sjölund, F. Sellberg - Proc. 1973 E.M.C. A.10.3. (Brussels,1973).

[17]. T.G. v.d. Roer, Proc. 1973, E.M.C. A.11.2. (Brussels, 1973).

[18]. A. Dascalu - IEEE Trans. ED-19, 1239-1251 (1972).

[19]. M.E. Hines - IEEE Trans. ED-13, 158-163 (1966).

[20]. W. Shockley, J.A. Copeland, R.P. James - in Quantum Theory of Atoms, Molecules and the Solid-State (P.O. Löwdin,ed.), 537-563, Ac.Press,N.York 1966.

[21]. M. El-Gabaly, J. Nigrin and P.A. Goud - J. Appl. Phys., 44, 4672-80.

[22]. C. Canali, G. Ottaviani, A. Alberighi Quaranta - J. Phys. Chem. Sol. 32, 1707-1720 (1971).

[23]. G. Björkman, C.P. Snapp - Electron. Lett. 8, 501-503 (1972).

CAPTIONS TO THE FIGURES

Fig. 1. Structure of a Baritt-diode.

Fig. 2. Field distributions at punch-through.

a. electric field.
b. electric potential.
c. energy-band diagram.

Fig. 3. Division of the diode into three regions:

I. contact region.
II. diffusion region.
III. drift region.

Fig. 4. Illustration of the impedance-field method.

Fig. 5. v-E-characteristics

——— measured by Canali et.al. [22] at room temperature

-.-.-. approximation by eq (64).

------ three-line approximation used in the calculations:

I. $v = \mu_o E$.
II. $\frac{dv}{dE} = \mu_2$.
III. $v = v_s$.

Fig. 6a. Comparison of calculated real admittance and noise figure with experiments (Björkman and Snapp [23]).

——— calculated

------ experimental

$I = 5mA$, $T = 17^oC$.

Fig. 6b. As 6a. $I = 20mA$, $T = 17^oC$.

Fig. 6c. As 6a. $I = 40mA$, $T = 17^oC$.

Fig. 7. Influence of the parameter E_i.

$I = 5mA$, $T = 17^oC$.

E_i in kV/cm is indicated at the curves.

Fig. 8a. Influence of diode temperature.

$I = 20mA$.

The temperature in degrees centigrade is indicated at the curves.

Fig. 8b. As 8a. $I = 40mA$.

Fig. 9. Influence of donor density.

$I = 20mA$, $T = 50^oC$.

N_D in 10^{15} cm^{-3} is indicated at the curves.

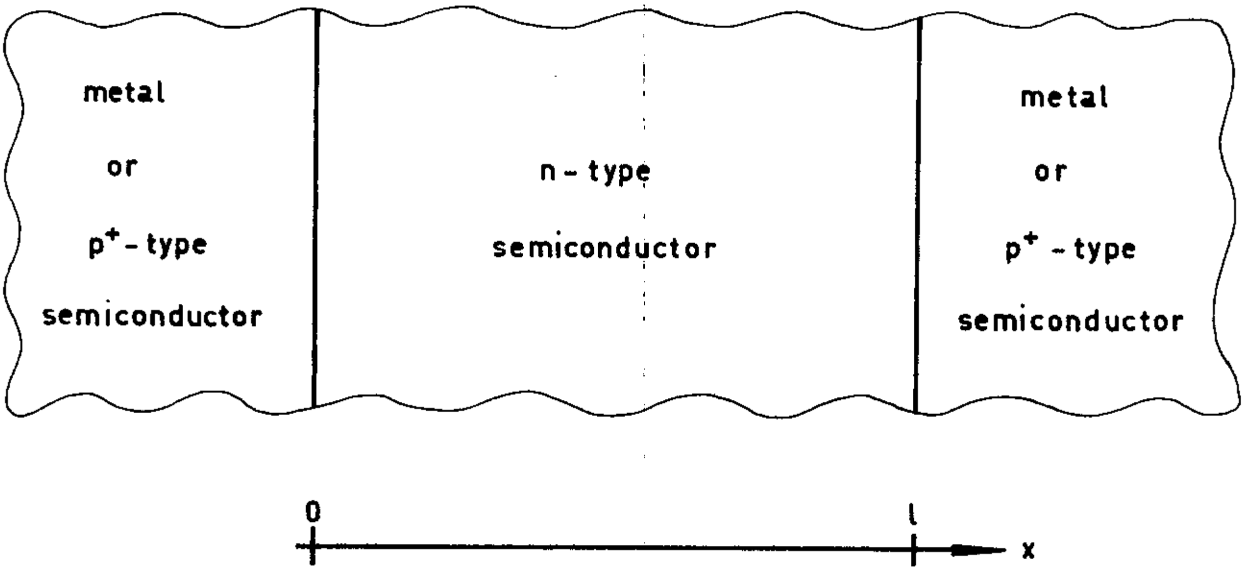
metal
or
p+ - type
semiconductor
n - type
semiconductor
metal
or
p+ - type
semiconductor
0
l
x

Fig. 1.

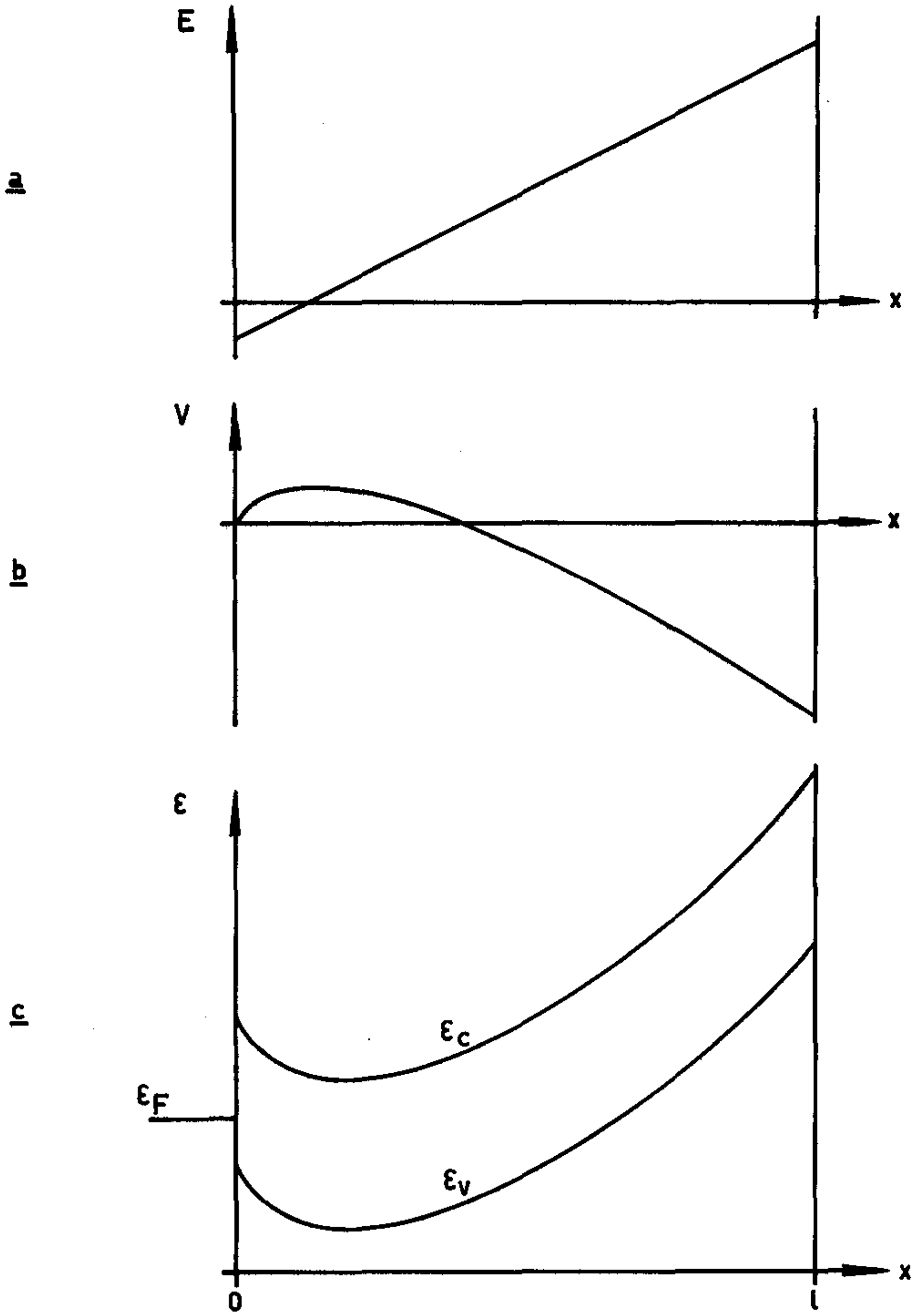

Fig. 2.

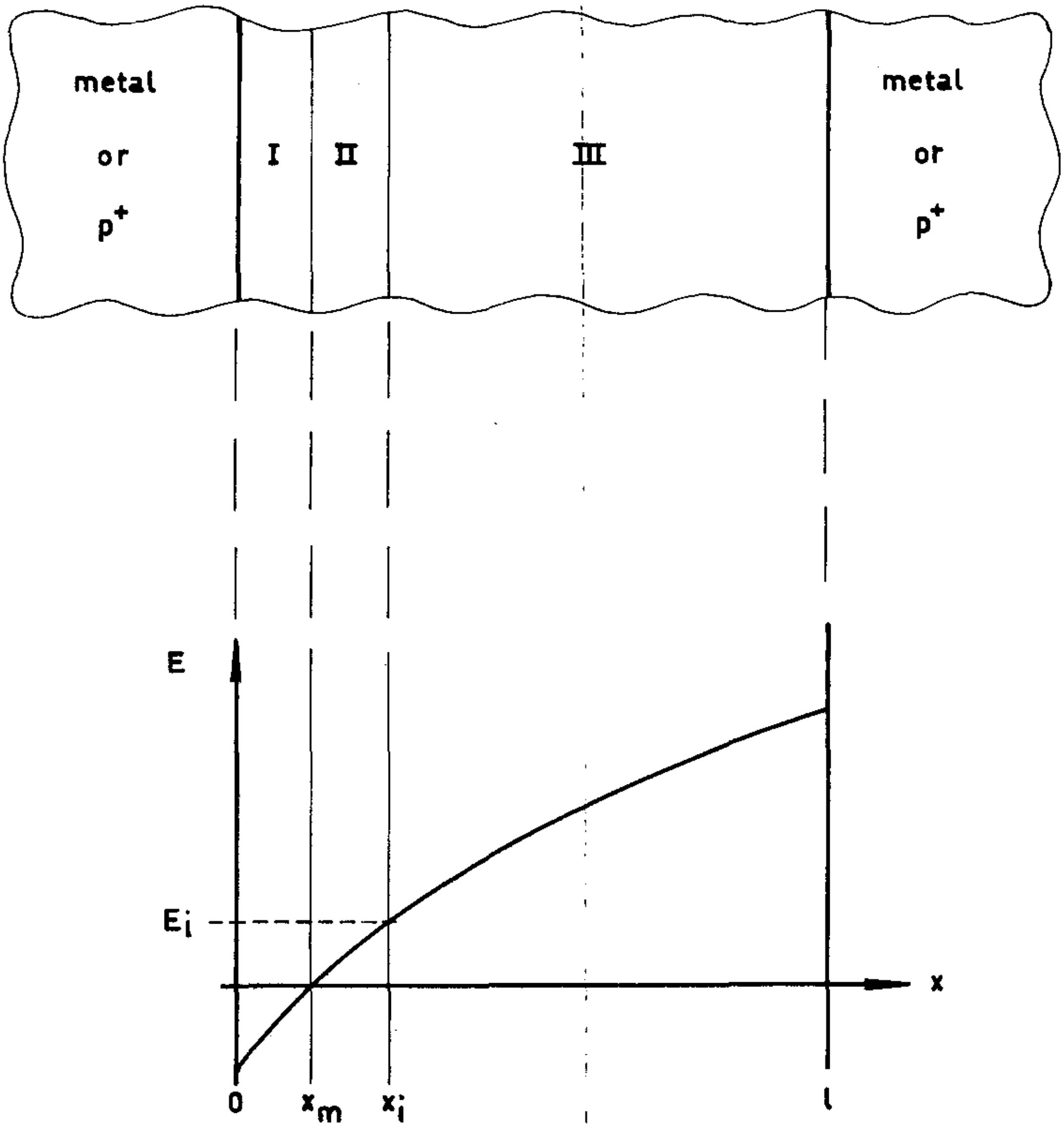

Fig. 3.

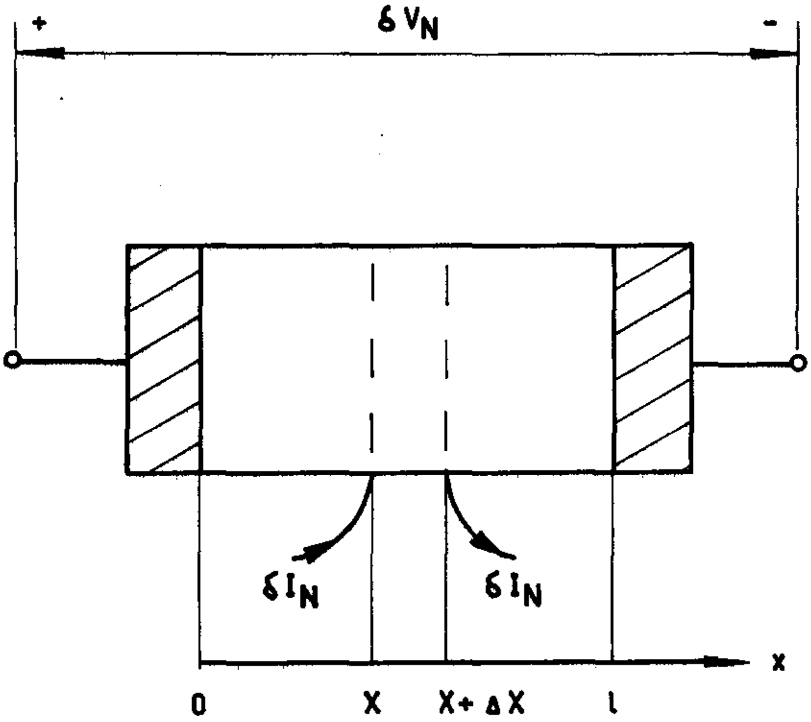

Fig. 4.

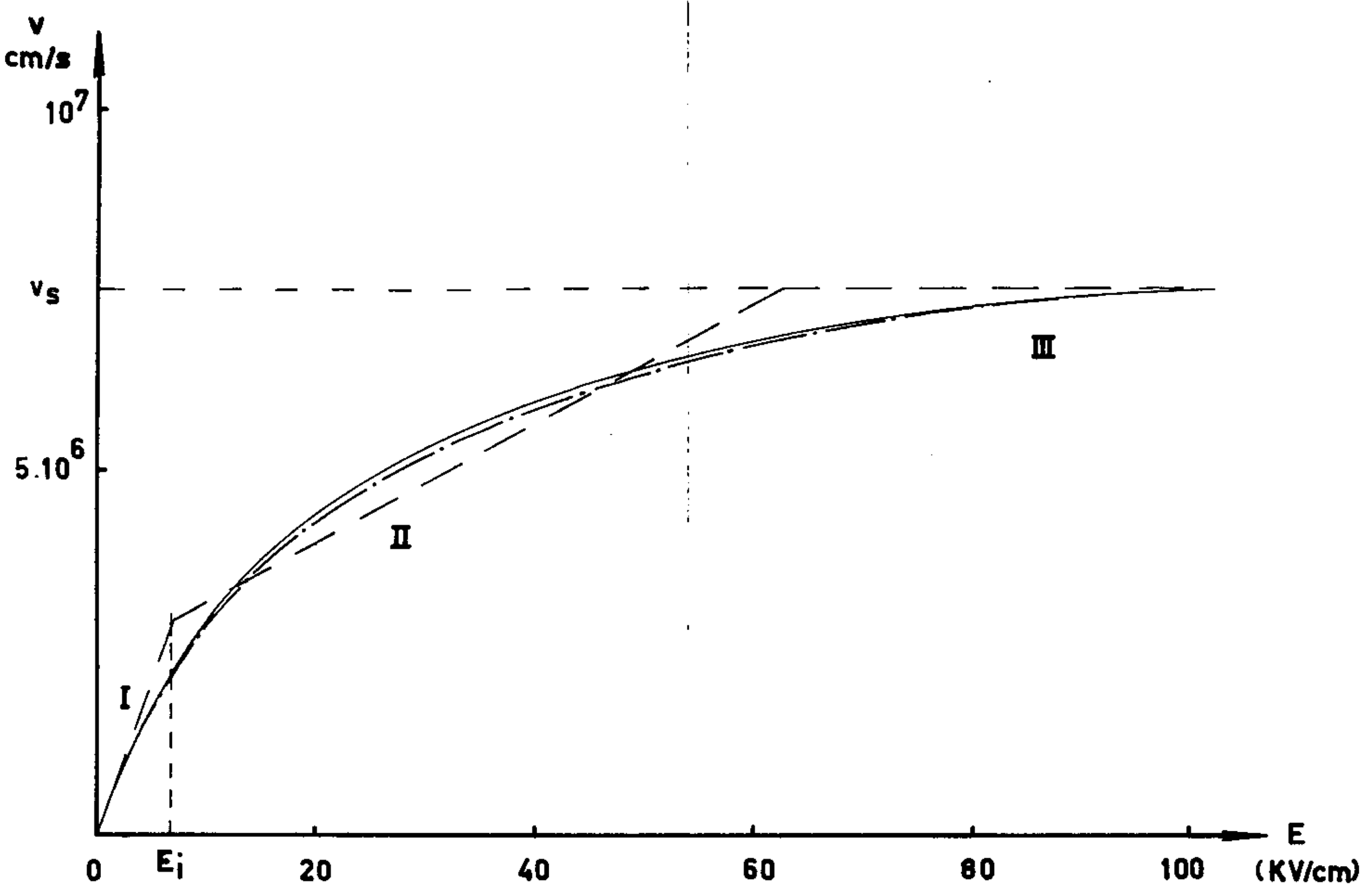

Fig. 5.

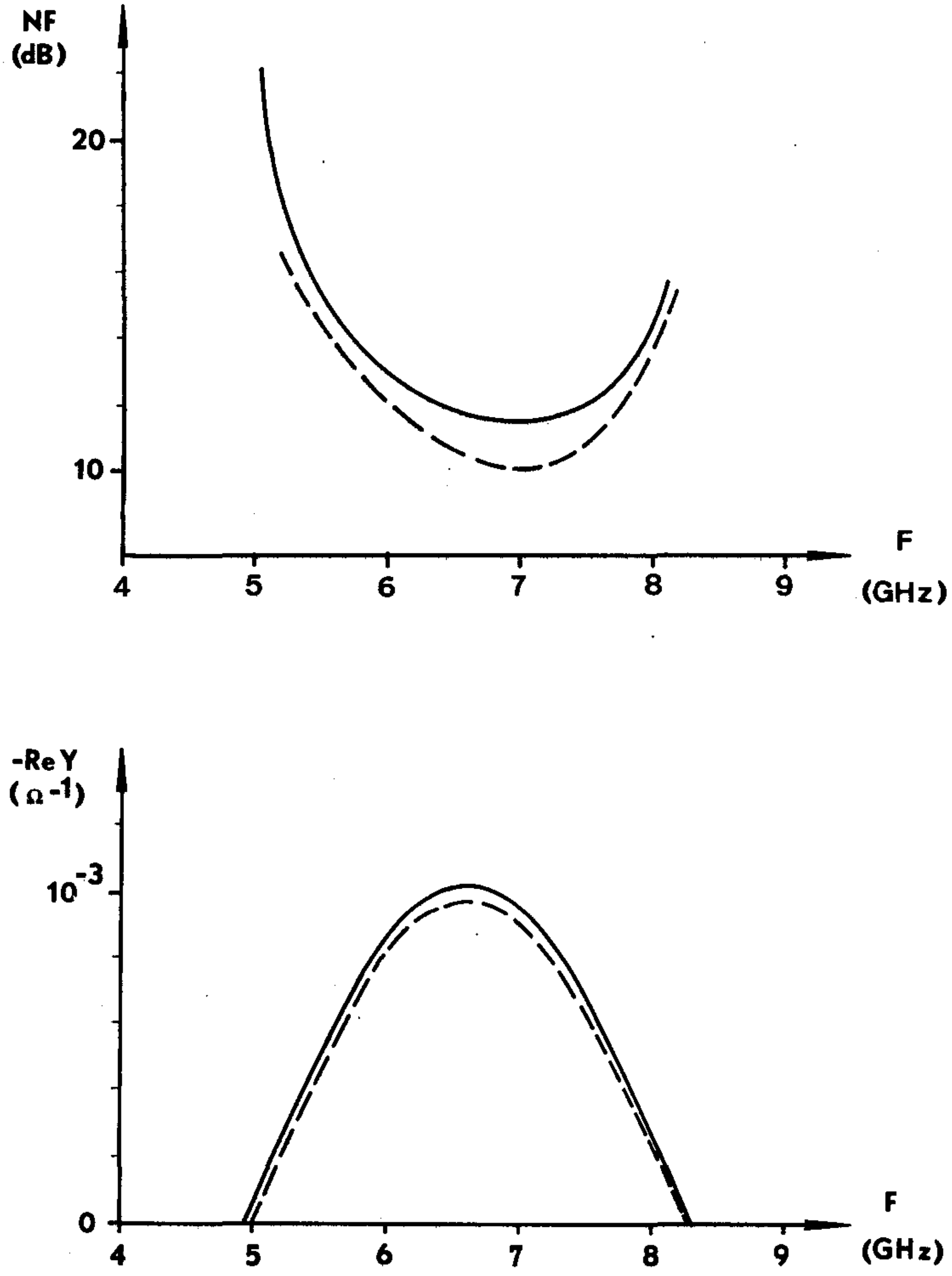

Fig. 6a.

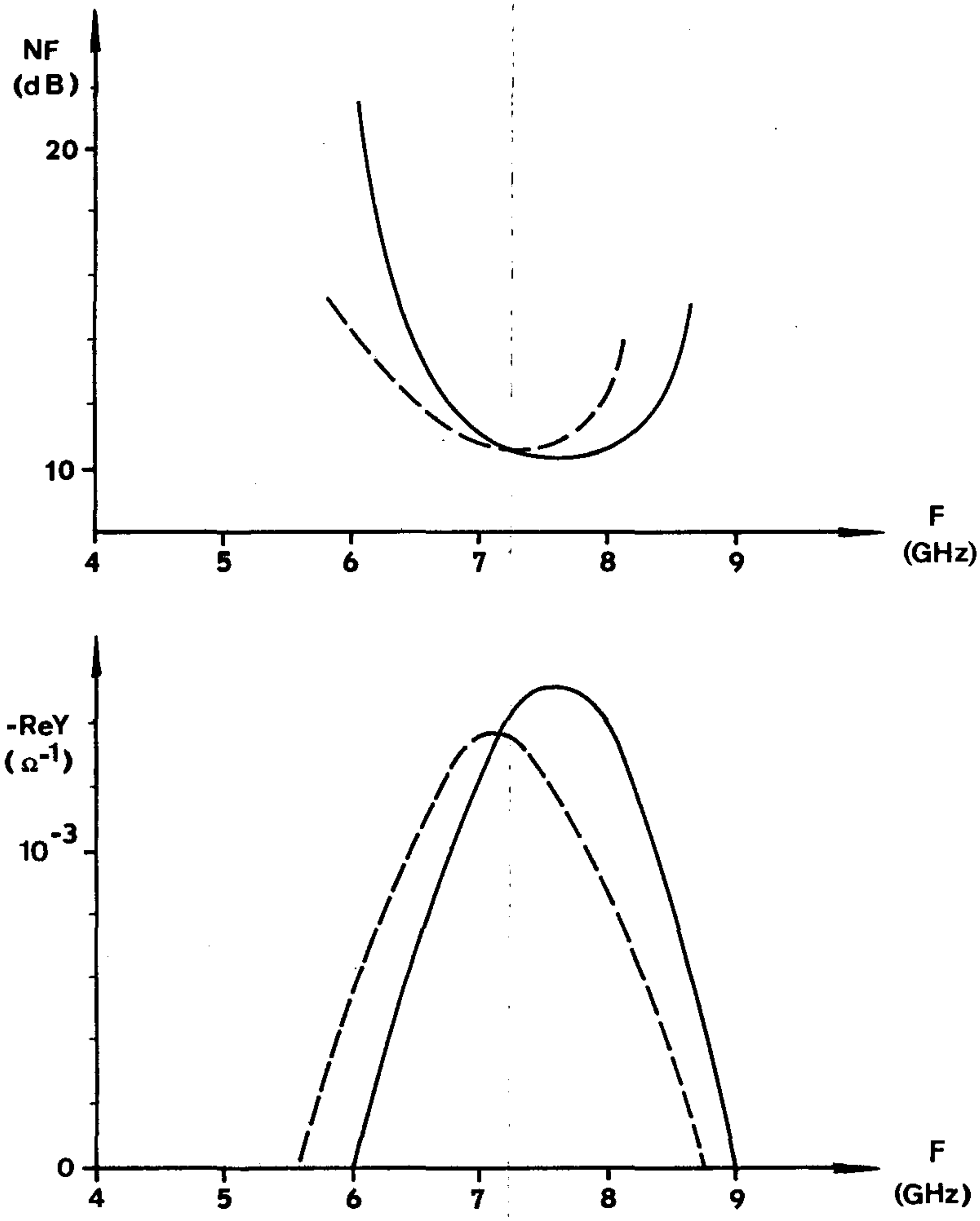

Fig. 6b.

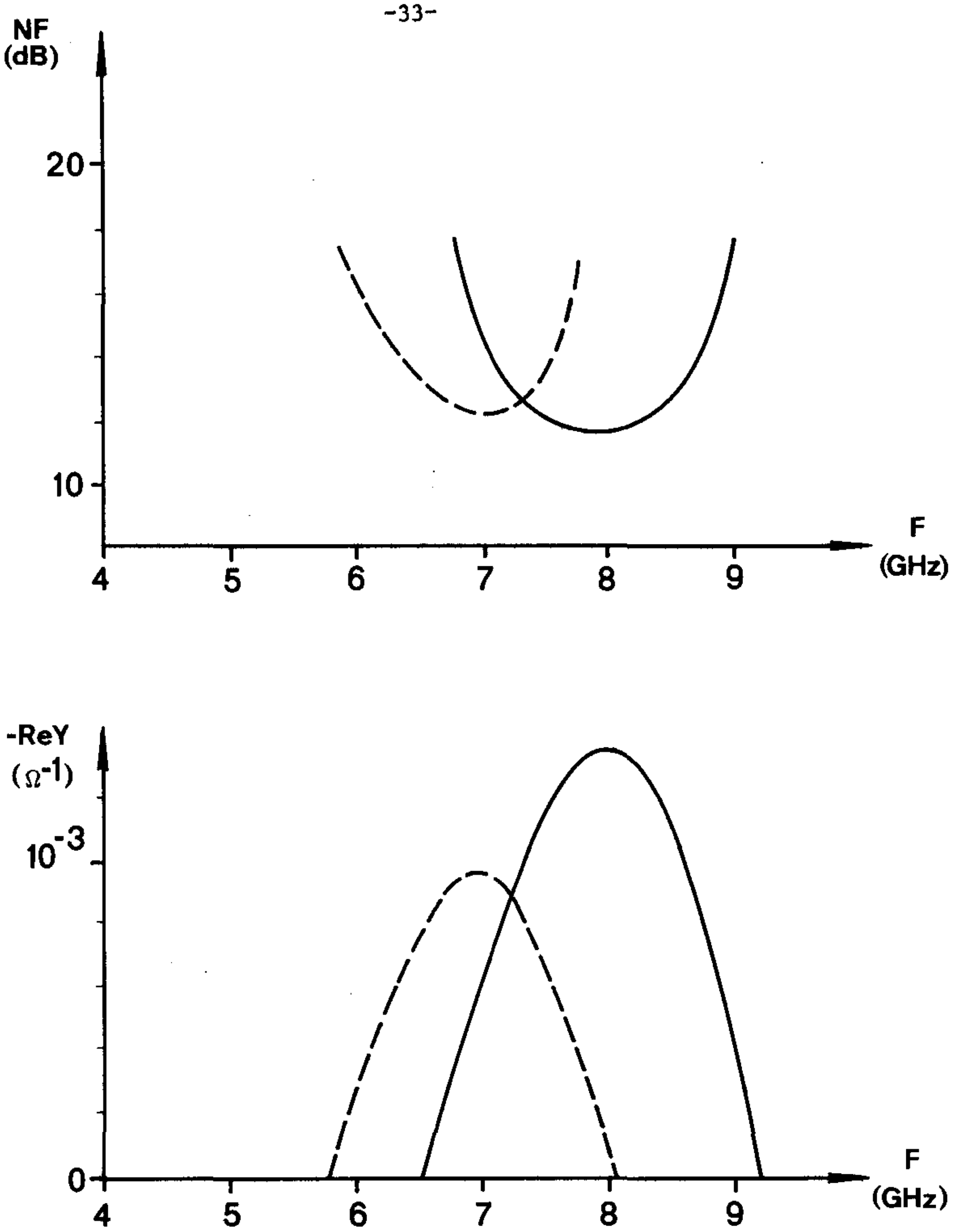

Fig. 6c.

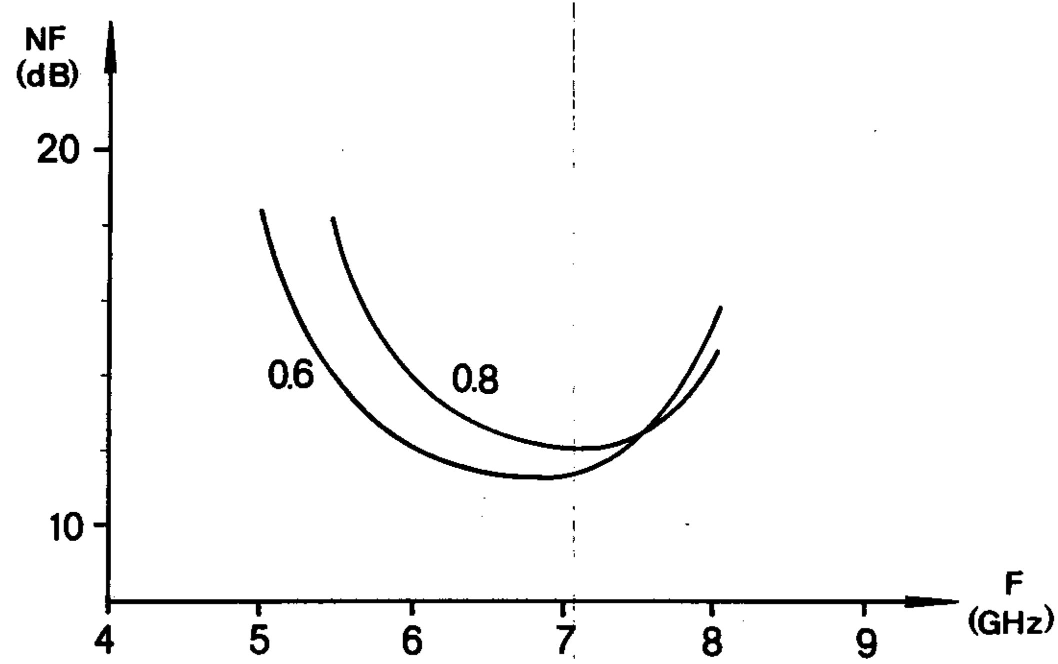

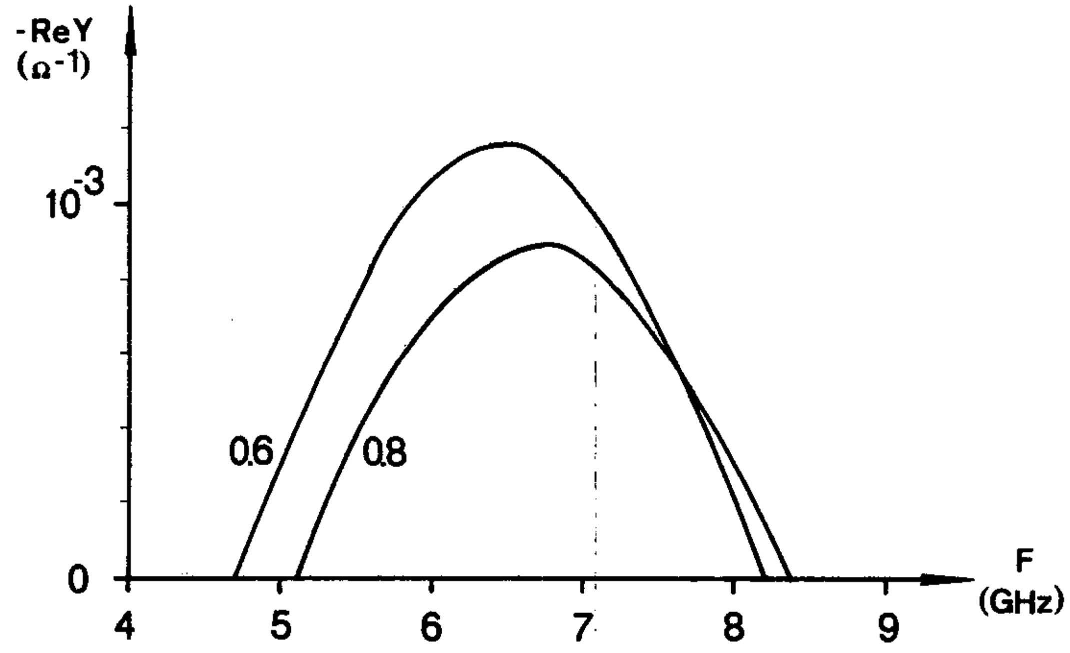

Fig. 7.

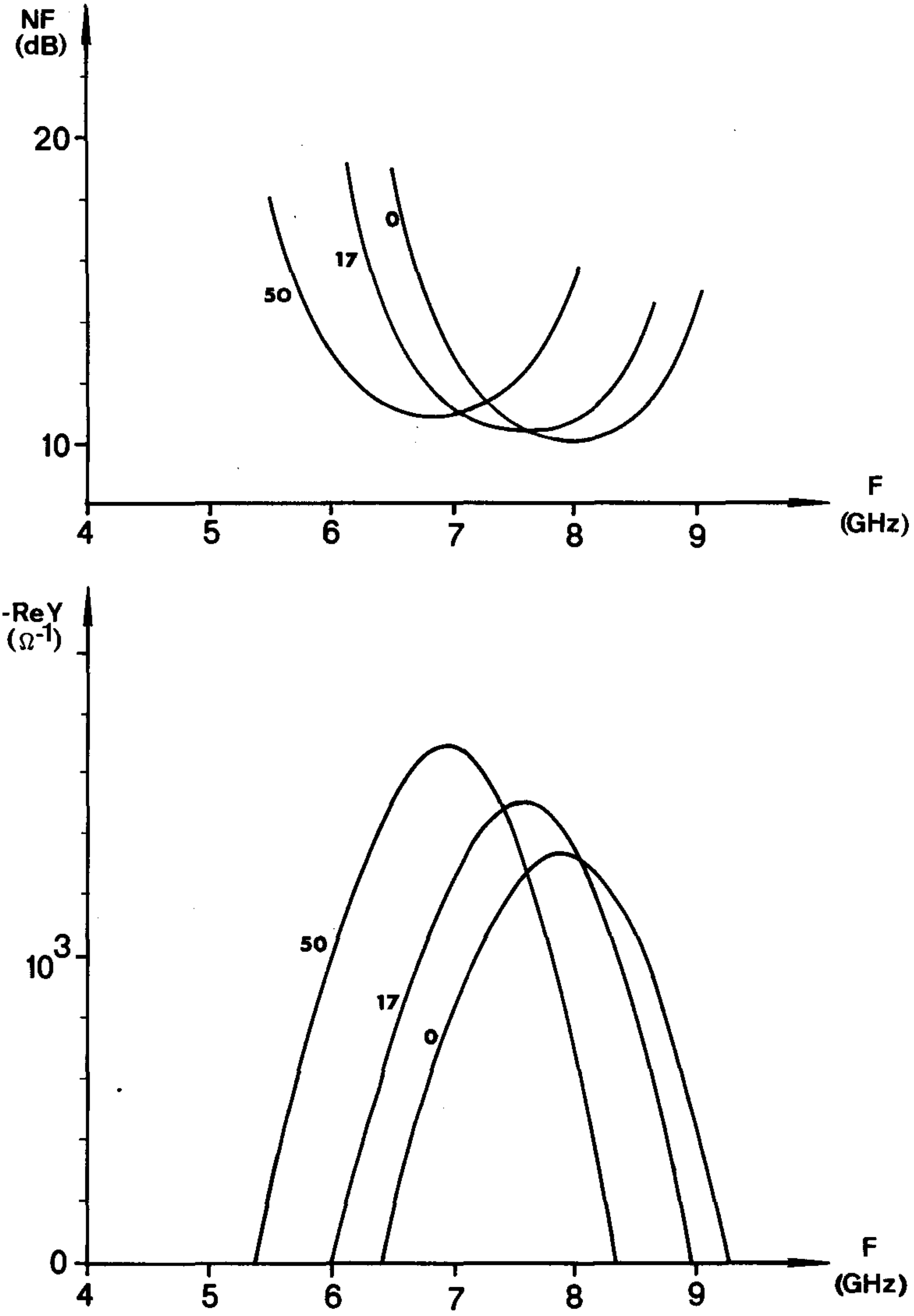
NF
(dB)
20
10
0
17
50
F
(GHz)
4
5
6
7
8
9
-ReY
(Ω^{-1})
10^3
50
17
0
0
F
(GHz)
4
5
6
7
8
9

Fig. 8a.

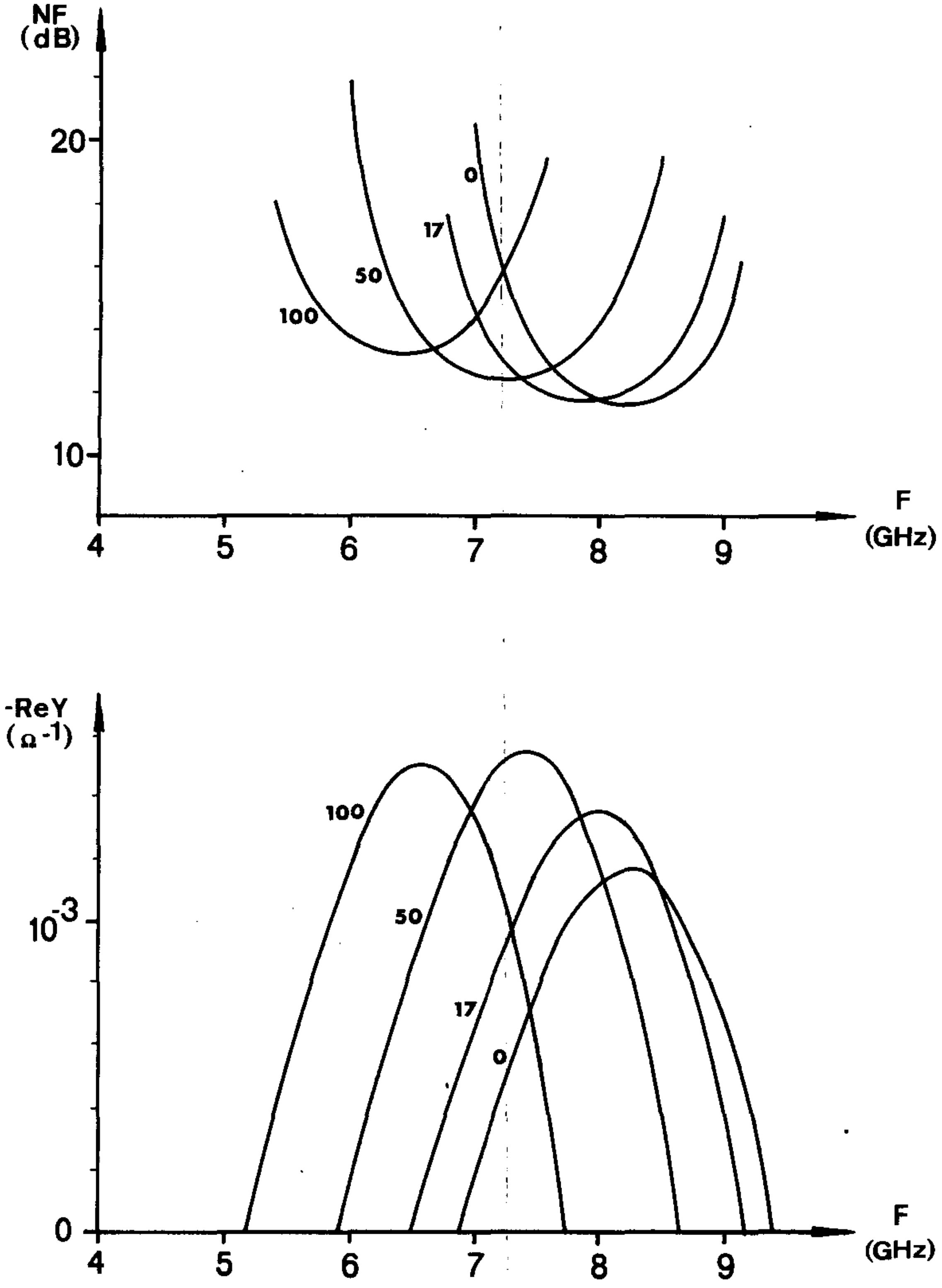
NF
(dB)
20
10
0
17
50
100
F
(GHz)
4
5
6
7
8
9
-ReY
(Ω^{-1})
10^{-3}
100
50
17
0
0
F
(GHz)
4
5
6
7
8
9

Fig. 8b.

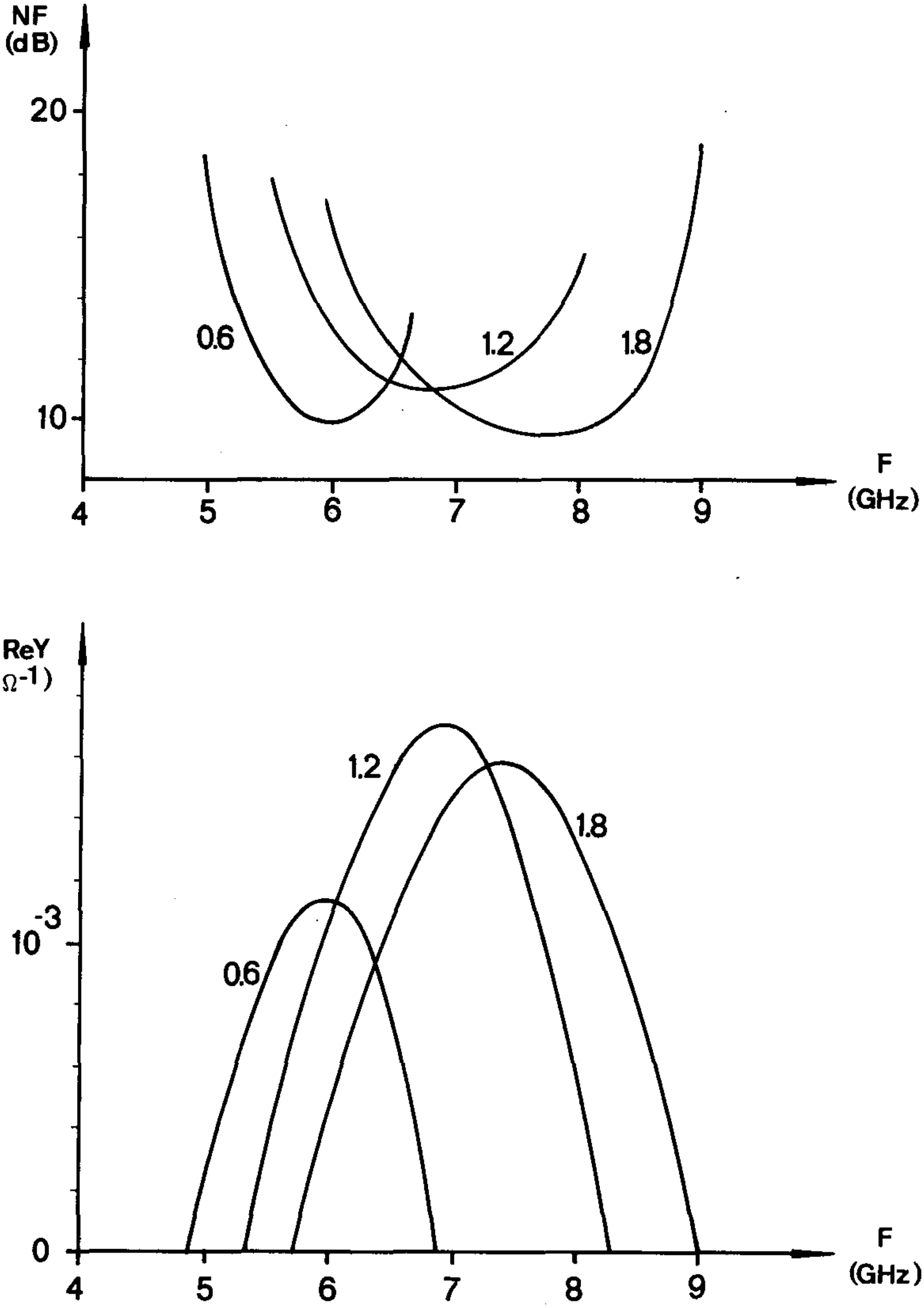

Fig. 9.

LIST OF SYMBOLS

Symbol	meaning	first on page
A	diode area	9
B_o, B_1, B_2	integration constant	11
C	" "	18
C_i	diffusion region capacitance	12
D	diffusion constant	11
E	electric field	6
E_i, E_s	parameter	6
e	elementary charge	6
F	auxiliary function	8
Δf	bandwidth	16
G	amplifier gain	15
I_s	noise current	16
δI_N	" "	17
i	reduced current density	6
i_o, i_1	d.c., a.c. components of i	7,8
i_s	reduced noise current	16
δi_t	" " "	18
J	current density	6
J_o, J_1	d.c., a.c. components of J	14 ,9
J_{so}	parameter	14
j	imaginary unit	6
k	Boltzmann's constant	14
ℓ	diode length	7
M	noise measure	15
N_D	donor concentration	6
N_v	valence band density of states	14
p	hole concentration	6
p_o	d.c. component of p	12
t	time	6
V	potential	14
V_s	shot noise voltage	19
V_T	thermal voltage	14
V_{th}	thermal noise voltage	17
V_{od}	d.c. voltage over drift region	7
V_{sd}	shot noise voltage, drift region	16
V_{si}	" " " , diffusion region	16
V_N	noise voltage, open circuit	15

δV_N	noise voltage	17
v	drift velocity	6
v_s	" " , saturated value	6
X	space coordinate	17
X_r	reduced value of X	17
x	space coordinate	6
x_i	beginning of drift region	7
x_m	potential maximum	fig. 3.
Z_o	normalizing impedance	9
Z_1	small-signal impedance	15
Z_c	impedance, contact region	15
Z_d	" , drift region	9
Z_i	" , diffusion region	12
Z_{TX}	transfer impedance	17
α	reduced frequency	6
γ_1,γ_2	propagation constants	11
δ	reduced diffusion constant	11
ε	dielectric constant	6
η	reduced electric field	6
η_o,η_1	d.c., a.c. component of η	7
η_{1h},η_o'	auxiliary variable	8
η_d	value of η at diode end	7
η_i	" " " " x_i	7
η_s	reduced noise field	16
ζ	parameter	14
λ_D	debye length	14
μ_o	low field mobility	6
ν	reduced drift velocity	6
ν_o,ν_1	d.c., a.c. component of ν	7
ν_o'	auxiliary variable	8
ν_i	parameter	9
ν_a	"	11
ξ	reduced space coordinate x	6,14
ξ_i	reduced value of x_i	7
ξ_ℓ	" " " ℓ	9
ξ_m	" " " x_m	11

ρ_i	parameter	8
σ	"	6
σ_c	"	12
τ	new coordinate	8
τ'	auxiliary variable	8
τ_ℓ	value of τ at ℓ	9
τ_x	auxiliary variable	19
ϕ	reduced potential	14
ψ'_m	potential barrier for holes	14
ω	angular frequency	6